Heliyon 10 (2024) e37935

Contents lists available at ScienceDirect

Heliyon

journal homepage: www.cell.com/heliyon

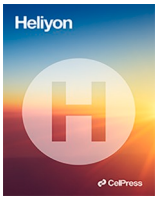

Research article

Anti-inflammatory Capacity of a Medicinal herb extract, *Anemarrhena asphodeloides*, on *In vivo* and *In vitro* models-induced atopic dermatitis

Hye-Min Kim [a,b], Yun-Mi Kang [b,c], Bo-Ram Jin [a], Minho Lee [d,**], Hyo-Jin An [a,e,*]

[a] *Department of Integrated Drug Development and Natural Products, Graduate School, Kyung Hee University, Seoul, 02447, Republic of Korea*
[b] *Department of Herbology, College of Korean Medicine, Sangji University, 83, Sangjidae-gil, Wonju-si, 26339, Republic of Korea*
[c] *Korean Medicine (KM)-Application Center, Korea Institute of Oriental Medicine (KIOM), 70 Cheomdan-ro, Dong-gu, Daegu, 41062, Republic of Korea*
[d] *Department of Life Science, Dongguk University-Seoul, Ilsandong-gu, Goyang-si, Gyeonggi-do, 10326, Republic of Korea*
[e] *Department of Oriental Pharmaceutical Science, College of Pharmacy, Kyung Hee University, Seoul, 02447, Republic of Korea*

ARTICLE INFO

Keywords:
Atopic dermatitis
Anemarrhena asphodeloides
TSLP
STAT
MAPK
TWEAK/FN14

ABSTRACT

Anemarrhena asphodeloides (AA) Bunge, a rhizomatous plant from the Liliaceae family, is traditionally utilized to manage inflammatory conditions. Nevertheless, its impact on atopic dermatitis (AD) and the associated molecular pathways have not yet been fully explored. This study explored the therapeutic effects of AA on AD both *in vivo*, using 2,4-dinitrofluorobenzene-induced NC/Nga mice, and *in vitro*, with tumor necrosis factor-α/interferon-γ-stimulated HaCaT keratinocytes. Topical application of AA ointment on the dorsal skin notably alleviated AD symptoms and skin lesions, enhanced the dermatitis score, and improved parameters such as the rate of transepidermal water loss, epidermal thickness, mast cell infiltration, systemic IgE levels, and cytokine expression. Furthermore, AA treatment significantly reduced serum levels of thymic stromal lymphopoietin (TSLP) and locally suppressed mRNA expression of thymus and activation-regulated chemokine (TARC) along with other relevant cytokines in affected skin. Both *in vivo* and *in vitro* applications of AA curtailed TSLP levels by inhibiting the expression of signal transducer and activator of transcription 6, a key regulator of pruritus and an initiator of mitogen-activated protein kinase signaling pathways. Additionally, AA affected the expression of tumor necrosis factor-like weak inducer of apoptosis/fibroblast growth factor-inducible 14, a pathway of interest in the study of cutaneous inflammatory diseases. Collectively, these findings propose that AA holds potential as an effective therapeutic agent for treating AD-induced skin inflammation.

Abbreviations: AA, Anemarrhena asphodeloides; AD, Atopic dermatitis; DNCB, 2,4-dinitrofluorobenzene; DEX, Dexamethasone; Fn14, Fibroblast growth factor-inducible 14; TNF-α/IFN-γ, Tumor necrosis factor-α and Interferon-γ; TWEAK, Tumor necrosis factor-like weak inducer of apoptosis; MAPK, Mitogen-activated protein kinase; TSLP, Thymic stromal lymphopoietin; STAT, Signal transducer and activator of transcription.

* Corresponding author. Department of Integrated Drug Development and Natural Products, Graduate School, Kyung Hee University, Seoul, 02447, Republic of Korea.
** Corresponding author.
E-mail addresses: mins7576@daum.net (H.-M. Kim), ymkang1013@kiom.re.kr (Y.-M. Kang), wlsqh92@gmail.com (B.-R. Jin), MinhoLee@dgu.edu (M. Lee), hjan@khu.ac.kr (H.-J. An).

https://doi.org/10.1016/j.heliyon.2024.e37935
Received 31 August 2023; Received in revised form 6 September 2024; Accepted 13 September 2024
Available online 19 September 2024

1. Introduction

Atopic dermatitis (AD) stands as a persistent inflammatory skin condition with a multifactorial origin, marked by pruritic eczematous lesions and a disrupted epidermal barrier. It manifests with symptoms including dryness, rash, erythema, scaling, edema, hemorrhage, and excoriations, arising from intricate interactions with allergens and various environmental, genetic, and immunological factors [1]. Prevalence statistics reveal that one in ten individuals grapple with AD, with more than a quarter of affected children experiencing a diminished quality of life, underscoring the imperative for effective AD management strategies. Dysfunctions in the skin barrier precipitate disruptions in pH balance, dehydration, and trans-epidermal water loss (TEWL), ultimately compromising the integrity and cohesion of the stratum corneum, thereby fostering dysregulated humoral immune responses typified by imbalances in T helper (Th)1/Th2-mediated cytokine equilibrium [2,3].

NC/Nga mice, developed in 1957, are a widely recognized *in vivo* model for AD, offering insights into AD pathogenesis. This inbred strain mirrors phenotypic characteristics akin to naturally occurring AD within typical environmental contexts. Exposure to various haptens or pathogens induces immunological alterations and barrier impairments akin to those observed in clinical dermatitis [4]. The allergenic compound 2,4-dinitrofluorobenzene (DNCB) provokes contact dermatitis and serves as a tool to probe skin dermatitis pathogenesis [5]. DNCB interacts with Langerhans cells, dermal dendritic cells, and macrophages, inciting Th cell differentiation via escalated serum levels of IgE and Th2 cytokines following repeated exposure [6].

The onset of AD correlates with immune cell hypersensitivity, encompassing keratinocytes, monocytes, dendritic cells, and eosinophils [7]. Keratinocytes, predominant in the epidermal cell population, secrete pro-inflammatory cytokines, immunoregulatory cytokines, and chemokines, thereby modulating Langerhans cell activity. Tumor necrosis factor (TNF)-α and interferon (IFN)-γ synergistically stimulate keratinocyte expression, activating diverse signaling cascades, including signal transducer and activator of transcription (STAT), mitogen-activated protein kinases (MAPKs), and nuclear factor-kappa B (NF-κB) pathways [8,9].

While topical corticosteroids like dexamethasone (DEX) are commonly employed to mitigate excessive immune response and inflammation in the clinical management of AD, they often carry significant risks of adverse effects and comorbidities. Examples include atrophoderma, telangiectasia, skin atrophy, rosacea, severe acne, and adrenal suppression [10]. Consequently, recent research has underscored the importance of exploring alternative therapeutic modalities, with a particular emphasis on identifying novel natural compounds for AD treatment [11].

Anemarrhena asphodeloides (AA) Bunge, a longstanding fixture in Chinese and Korean traditional medicine, has garnered attention for its potential therapeutic properties. Its rhizome has been historically employed in the treatment of various inflammatory ailments and is recognized for its antipyretic, sedative, diuretic, and antitussive effects [12]. Notably, several constituents isolated from AA exhibit promising pharmacological activities. For instance, AAP70-1, a novel polysaccharide derived from AA, has demonstrated neuroprotective effects through the attenuation of apoptosis and immunomodulatory actions [13]. Mangiferin, another compound isolated from AA, has been shown to possess anti-photoaging properties by suppressing matrix metalloproteinase-9 and promoting skin regeneration, epidermal thickening, and collagen fiber repair [14]. Moreover, clinical studies have highlighted the efficacy of timosaponin A-III, a principal chemical constituent of AA, in reducing wrinkle parameters in human skin [15]. Additionally, AA extracts, particularly Volufiline™, have found application as raw materials for enhancing skin elasticity and as ingredients in anti-wrinkle cosmetics, with no discernible impact on hormone balance.

Despite accumulating evidence from experimental and clinical studies suggesting the involvement of AA in enhancing skin barrier function and ameliorating inflammation, its efficacy as a treatment for AD remains uncertain. Hence, this study aims to investigate AA as a potential candidate for AD treatment, evaluate its effectiveness in alleviating AD-like symptoms, and elucidate underlying mechanisms via the DNCB-induced AD mouse model and TNF-α/IFN-γ-stimulated HaCaT keratinocytes.

2. Results

2.1. AA ameliorating AD skin lesions and clinical severity in vivo model

The experimental procedure is illustrated in Fig. 1A. DNCB induction triggers AD type skin lesions, with repeated local application exacerbating symptoms such as edema, dryness, erythema, excoriation, pruritus, and lichenification. In comparison to the Normal group, the DNCB group showed a marked increase in the manifestation of physical signs of AD. Conversely, the AA-treated groups (at doses of 50 and 100 mg/kg) demonstrated a reduction in AD symptom severity compared to the DEX group. Representative dorsal images and dermatitis scores depicted disease progression and mitigation (Fig. 1B and C). To assess the impact of AA on skin barrier function, we conducted weekly measurements of TEWL, summarizing the results on the last day of the study. The DNCB-treated group displayed an elevation in TEWL scores, whereas the AA group exhibited a decrease in TEWL scores (Fig. 1D). Spleen and lymph node weights were measured to evaluate the potential influence of AA treatment on systemic immune responses. Dysregulated immune responses in AD patients often manifest as splenomegaly and lymphadenopathy [16]. AA treatment mitigated DNCB-induced enlargement of the spleen and lymph nodes (Fig. 1E and F). The DEX-treated group, serving as a positive control, did not show splenic or lymph node hypertrophy, indicating appropriate drug dosage and duration without ethical concerns. Spleen and lymph node weights were normalized to body weight. Weekly body weight measurements indicated slight increases, with no significant differences between the AA-treated and the normal groups (data not shown). However, the DEX-treated group exhibited decreased body weight, indicative of growth retardation, a known side effect of prolonged DEX use. Collectively, these findings suggest that AA administration alleviates AD clinical symptoms *in vivo*.

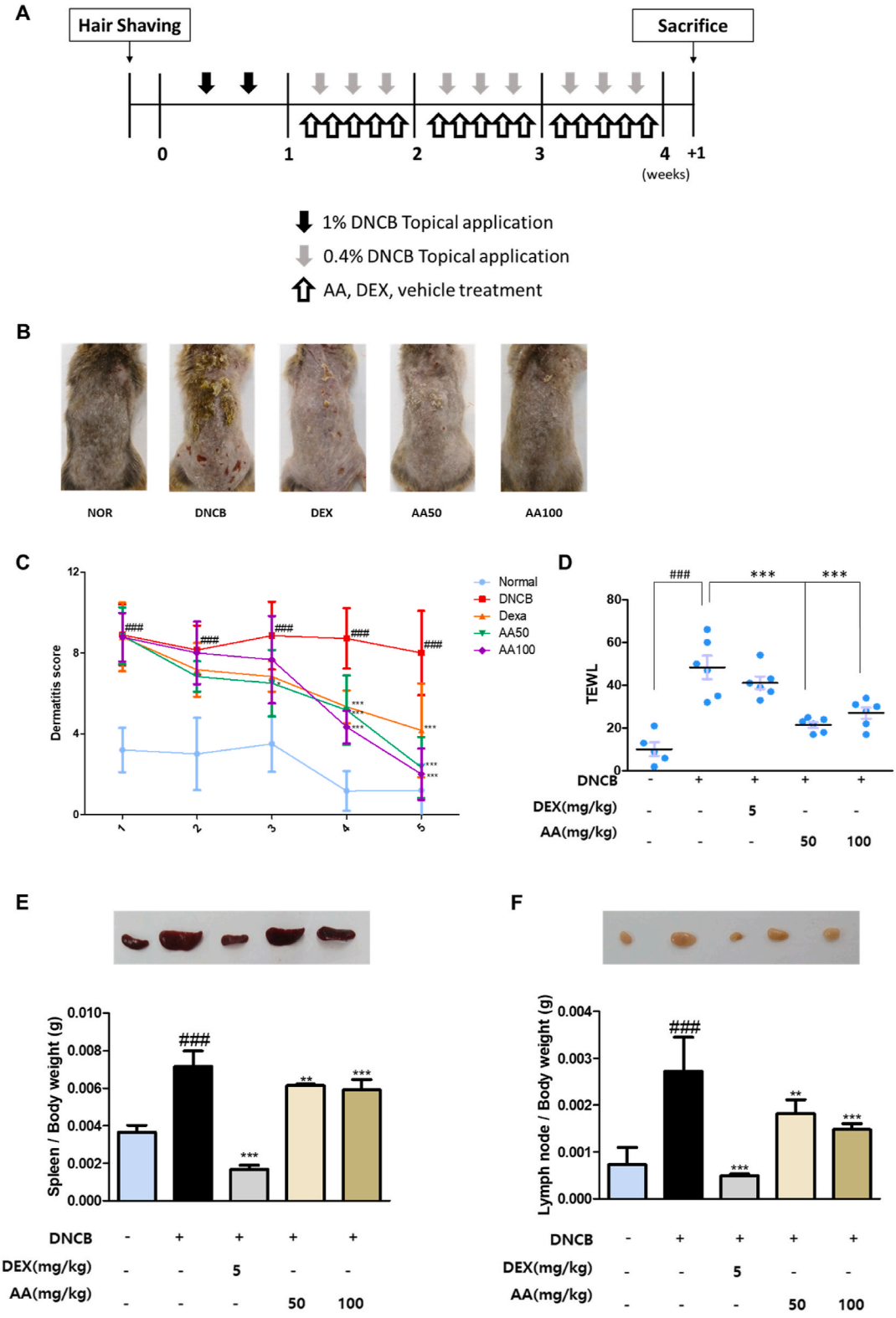

Fig. 1. Experimental procedure and impact of AA on the progression of atopic dermatitis in DNCB-induced NC/Nga mice.
(A) Schematic diagram of the animal experiment timeline. To induce AD-like skin inflammation, 200 μL of 1 % DNCB was applied twice for one week, followed by 150 μL of 0.4 % DNCB applied three times a week for four weeks. Mice were treated with DEX (5 μM, positive control) or AA (50, 100 mg/kg) daily for four weeks. (B) Clinical features of dorsal skin lesions. (C) Dermatitis scores were evaluated weekly as the sum of score for five

clinical index: dryness, edema, erosion, erythema and lichenification. (D) TEWL levels were recorded on the final day of the study. (E–F) Representative images illustrating the spleen and lymph node sizes and weights were taken at the conclusion of the experiment. Data are presented as the mean ± standard deviation from three independent experiments. Statistical significance was determined as follows: $^{###}p < 0.001$ vs. the control group; $^{**}p < 0.01$ and $^{***}p < 0.001$ vs. DNCB-treated group.

2.2. AA attenuating histological alterations and mast cell infiltration in vivo model

Atopic skin lesions are characterized by epithelial hyperplasia and hyperkeratosis. Histological analysis was conducted using H&E staining. The AA-treated groups exhibited a decrease in ear epidermal thickness (Fig. 2A) and dorsal skin thickness (Fig. 2B), akin to observations in the positive control group. Similarly, reductions in dermal thickness of ear tissue were evident in the AA-treated groups (Fig. 2D). To evaluate inflammatory cell infiltration in the skin, mast cell counts were performed on dorsal skin tissue sections using TB staining. DNCB application prompted mast cell accumulation, whereas AA treatments notably diminished mast cell numbers in dorsum skin compared to the DEX-treated group (Fig. 2C and F). Collectively, these findings suggest that AA administration mitigated histological manifestations of AD recurrence *in vivo*.

2.3. AA treatment suppressing the levels of immunoglobulin and cytokine production in vivo model

To evaluate the expression of inflammatory markers, we conducted ELISA and qRT-PCR analyses. Elevated levels of IgE and inflammatory cytokines are hallmark features of AD. The DNCB-treated group exhibited significantly increased serum IgE and TSLP levels, whereas AA-treated groups showed decreased expression levels (Fig. 3A and C). Additionally, dorsal protein levels of IL-6, a representative pro-inflammatory cytokine associated with Th2-mediated responses, were suppressed by AA treatment (Fig. 3B). Furthermore, mRNA levels of IL-4 and IL-13, typical Th2- associated cytokines, were decreased in the AA-treated groups compared to

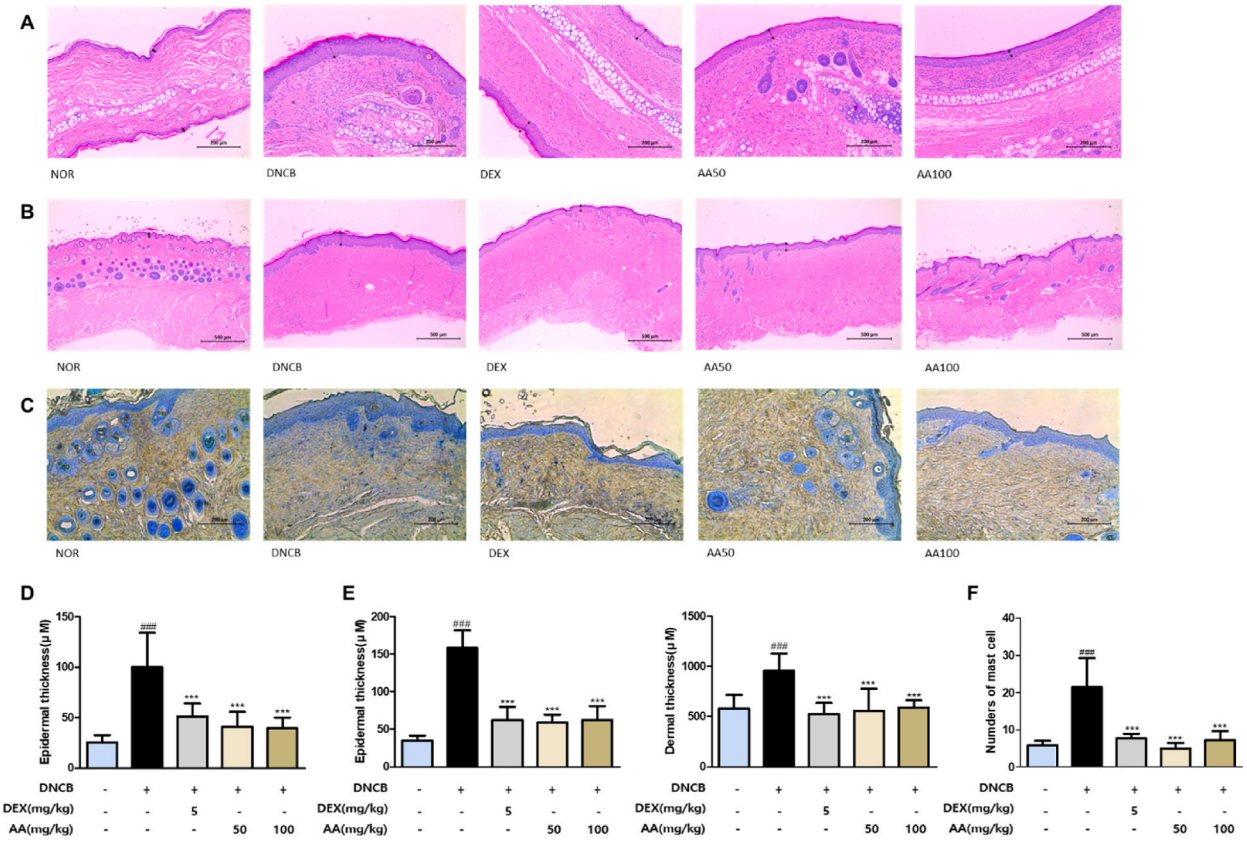

Fig. 2. Inhibitory impact of AA on histologic symptoms of AD in DNCB-induced NC/Nga mice. (A–B) Histological features of ear and dorsal skin by hematoxylin and eosin staining. (C) Histological features of dorsal skin by toluidine blue staining. (D) Epidermal thickness of the ear skin was measured. Scale bar = 200 μM. (E) The thickness of the epidermal and dermal dorsum skin was measured. Scale bar = 500 μM. (F) The infiltration number of mast cell was counted from randomly selected areas per mouse. Mast cells stained purple and averaged (n = 6). Scale bar = 200 μM. Data are presented as the mean ± standard deviation from three independent experiments. Statistical significance was determined as follows: $^{###}p < 0.001$ vs. the control group; $^{***}p < 0.001$ vs. DNCB-treated group. (For interpretation of the references to color in this figure legend, the reader is referred to the Web version of this article.)

negative control (Fig. 3D and E). Moreover, the mRNA level of TARC was elevated by DNCB treatment but attenuated by AA treatment (Fig. 3F). Similar changes in cytokine levels, except for IgE, were observed in the DEX-treated group. Overall, these findings underscore the regulatory effects of AA treatment on IgE and cytokine production in an *in vivo* model, culminating in AD inhibition.

2.4. AA regulating the expression of NF-κB, MAPK pathways-related factors, and STAT6/TSLP in vivo model

To conclusively establish the inhibitory effect of AA and elucidate the underlying mechanisms associated with AD inflammatory responses, we conducted *in vivo* protein expression analysis via western blotting. Regarding MAPK activation, pivotal for cytokine and chemokine production induction, AA treatment notably activated the ERK/JNK pathway. Phosphorylation of ERK and JNK, augmented by DNCB irritation, was attenuated by AA treatment (Fig. 4C). After MAPK phosphorylation, IκB phosphorylation, crucial for NF-κB nuclear translocation, was diminished by AA treatment. Notably, IκB total expression, reduced in the DNCB irritation, was restored in both control and AA groups (Fig. 4B). Additionally, TAK1 phosphorylation, an upstream regulator in these pathways, was heightened with DNCB treatment but subdued with AA treatment (Fig. 4A). TSLP, implicated in mast cell activation and allergic inflammation exacerbation, is stimulated by STAT6 [17]. DNCB treatment induced elevated expression of p-STAT6 and TSLP, both attenuated by AA treatment (Fig. 4D). In sum, these findings indicate that AA treatment exerts anti-atopic effects by suppressing NF-κB, MAPK pathways, STAT6, and TSLP *in vivo*.

Protein levels were assessed via Western blot analysis using specific antibodies, with β-actin serving as the internal control. The quantification of protein expression was performed by measuring the band intensity relative to the corresponding total protein form. (A) Protein levels of the phosphorylation TAK1. (B) Protein levels of the phosphorylation IκB. (C) Protein levels of the phosphorylation ERK and JNK. (D) Protein levels of the phosphorylation of STAT6 and TSLP. Data are presented as the mean ± standard deviation from three independent experiments. Statistical significance was determined as follows: $^{###}p < 0.001$ vs. the control group; $^{***}p < 0.001$ vs. DNCB-treated group.

2.5. AA suppressing the TNF-α and TSLP production in vitro model

To elect the extent of the AA treatment effect in HaCaT keratinocytes, the cells were exposed to AA extracts at concentrations ranging from 15.6 to 1000 μg/mL for 24 h. No significant changes were observed in the survival rate of HaCaT cells regardless of the presence or absence of AA (Fig. 5A). The TNF-α/IFN-γ-stimulated cells showed significantly intensified expression levels of TNF-α and

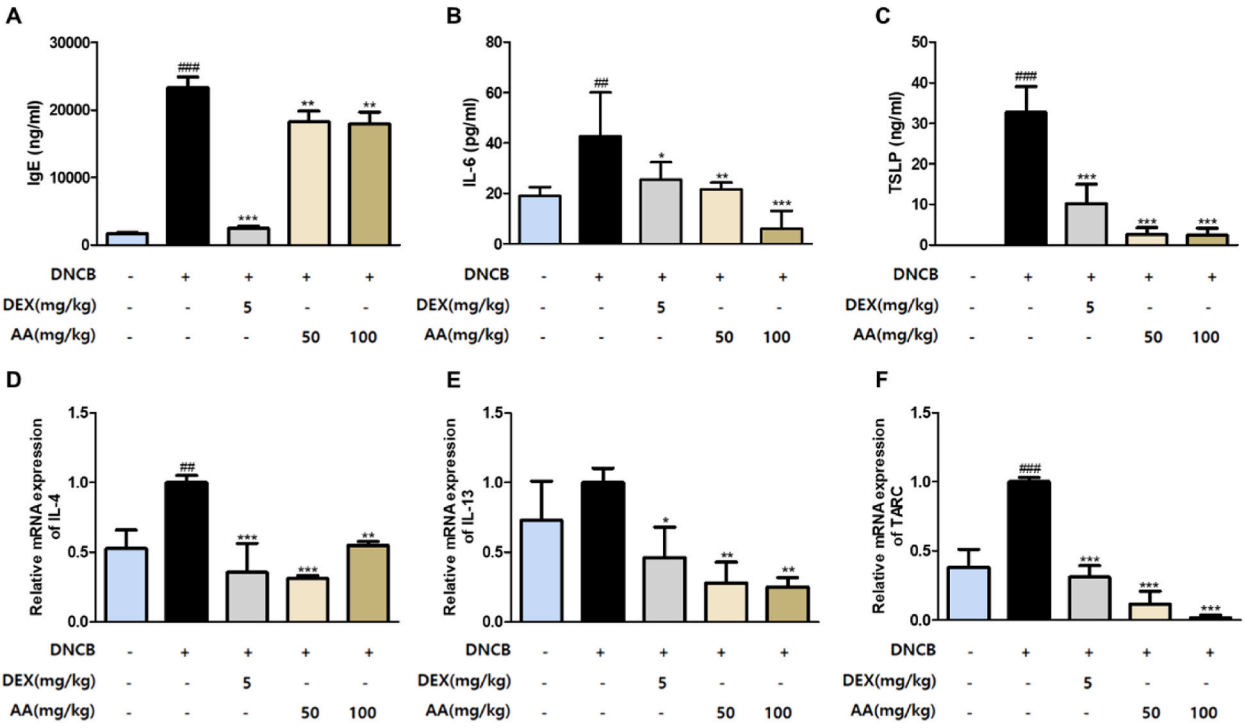

Fig. 3. Impact of AA on the expression of inflammatory cytokines and IgE production in DNCB-induced NC/Nga mice.
(A) Serum IgE levels, (B) IL-6 levels in dorsal skin protein, and (C) TSLP levels in serum were assessed using ELISA. Total RNA was extracted from dorsal skin samples. The gene expression of pro-inflammatory cytokines, (D) IL-4, (E) IL-13, and (F) TARC, were analyzed by qRT-PCR. Data are presented as the mean ± standard deviation from three independent experiments. Statistical significance was determined as follows: $^{##}p < 0.01$, $^{###}p < 0.001$ vs. the control group; $^{*}p < 0.05$, $^{**}p < 0.01$, and $^{***}p < 0.001$ vs. DNCB-treated group.

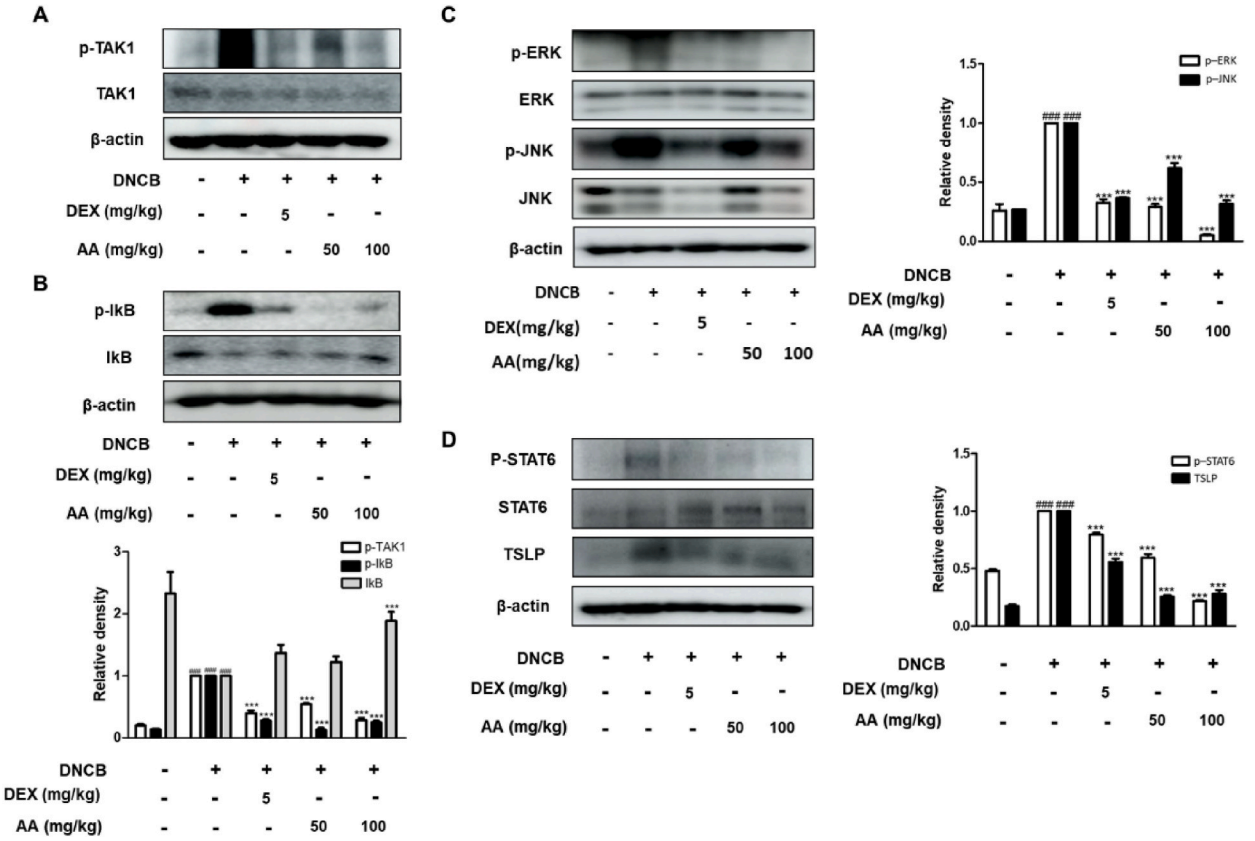

Fig. 4. Impact of AA on protein expression of AD-related signal pathways in DNCB-induced NC/Nga mice.

TSLP, while the AA-treated groups (100, 200, and 400 μg/mL) decreased both (Fig. 5B and C). Overall, these results reveal that TNF-α and TSLP in the *in vitro* model were regulated by AA administration, resulting in the inhibition of AD.

2.6. AA modulating the expression of NF-κB, MAPK pathways-related factors, STAT6/TSLP, and filaggrin in vitro model

To comprehensively investigate AA's inhibitory effects and elucidate the mechanism underlying AD inflammatory responses, we integrated *in vitro* and *in vivo* findings. Enhanced phosphorylation levels of TAK1 and IκB induced by TNF-α/IFN-γ treatment were mitigated by AA treatment. Notably, while IκB total expression increased in the control group, significant elevation was surveyed only in the high-concentration AA group (Fig. 6A and B). Phosphorylation of ERK, JNK, and SEK1/MKK4 escalated upon TNF-α/IFN-γ

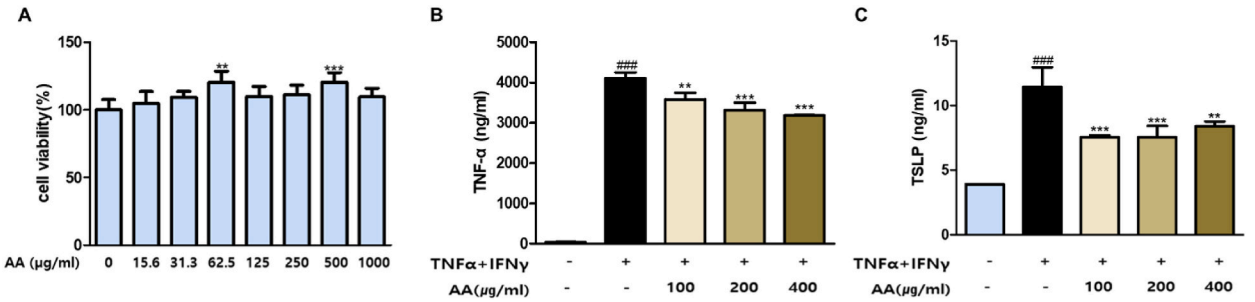

Fig. 5. Impact of AA on the production of inflammatory cytokines expression in TNF-α/IFN-γ-stimulated HaCaT Keratinocytes.
HaCaT cells were exposed to varied concentrations of AA for 24 h. (A) HaCaT cytotoxicity was determined using the MTT assay. The production of inflammatory cytokines, (B) TNF-α and (C) TSLP, was measured by ELISA using in the culture supernatants from cells treated with AA (100, 200, and 400 μg/mL) and TNF-α and IFN-γ (each 10 ng/mL) for 24 h. Data are presented as the mean ± standard deviation from three independent experiments. Statistical significance was determined as follows: $^{###}p < 0.001$ vs. the control group; $^{**}p < 0.01$, and $^{***}p < 0.001$ vs. TNF-α/IFN-γ-stimulated group.

exposure. AA treatment notably restrained p-ERK levels compared with TNF-α/IFN-γ exposure. Similarly, all groups treated with AA manifested diminished p-JNK levels compared to the negative control. Furthermore, AA treatment elicited concentration-dependent suppression of SEK1/MKK4 phosphorylation, an upstream regulator of p-JNK (Fig. 6C). Expression of p-STAT6 and its downstream effector, TSLP, increased following TNF-α/IFN-γ stimulation but decreased upon AA treatment (Fig. 6D). Additionally, filaggrin, crucial for maintaining skin barrier integrity, was suppressed by TNF-α/IFN-γ treatment but restored by AA treatment (Fig. 6E). Overall, these findings suggest that AA treatment mitigates inflammatory responses through modulation of the MAPK-related signaling pathway, STAT6/TSLP axis, and filaggrin expression *in vitro*.

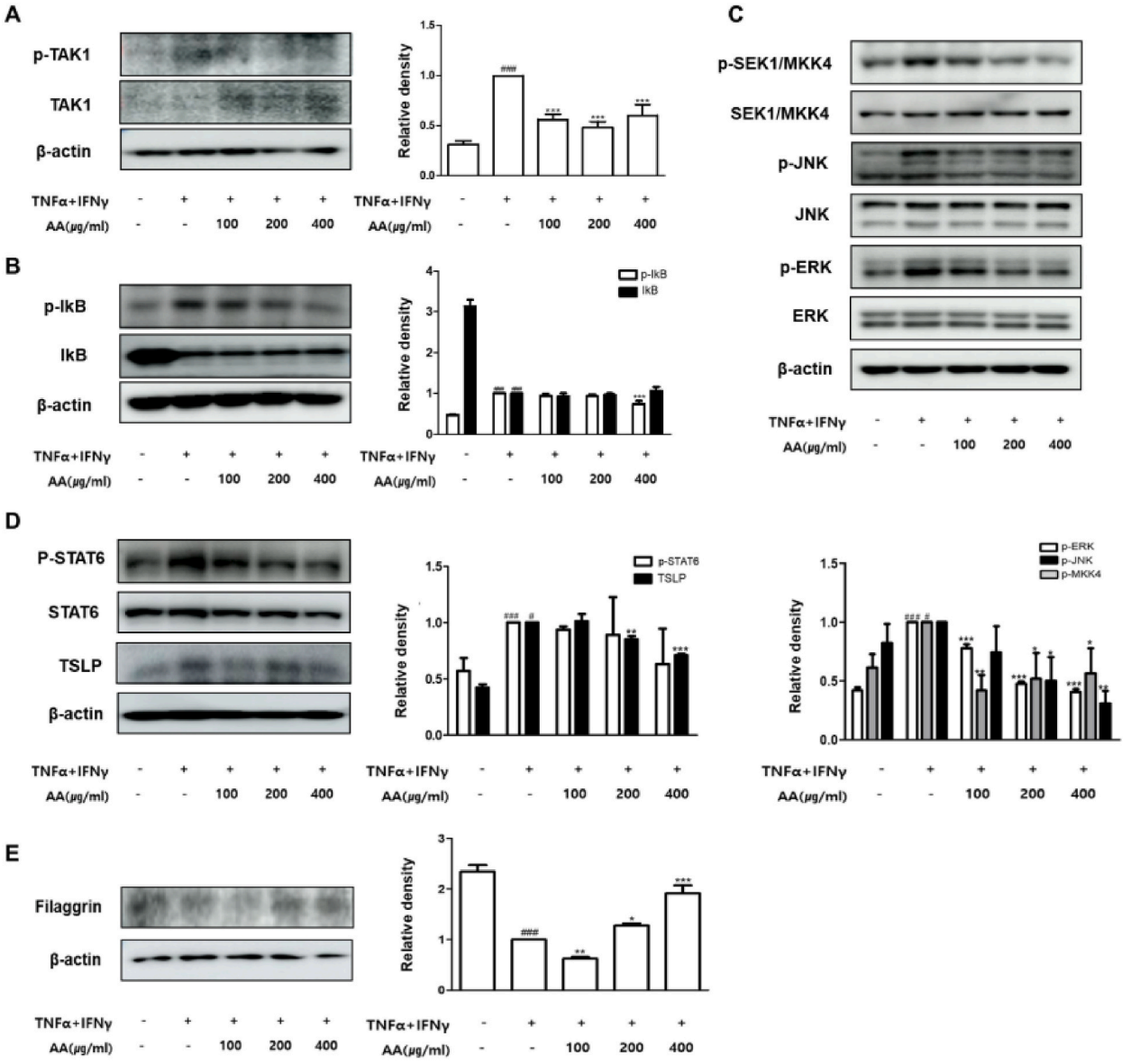

Fig. 6. Impact of AA on protein expression of AD-related signal pathways in TNF-α/IFN-γ-stimulated HaCaT Keratinocytes.
HaCaT cells were pre-treated with 100, 200, and 400 μg/mL of AA for 1 h prior to the addition of TNF-α/IFN-γ. The protein levels were assessed via Western blot analysis using specific antibodies, with β-actin serving as the internal control. The quantification of protein expression was performed by measuring the band intensity relative to the corresponding total protein form. (A) Phosphorylation of TAK1. (B) Phosphorylation of IκB. (C) Phosphorylation of ERK, JNK and SEK1/MKK4. (D) Phosphorylation of STAT6 and expression of TSLP. (E) The expression of Filaggrin. Data are presented as the mean ± standard deviation from three independent experiments. Statistical significance was determined as follows: $^{###}p < 0.001$ vs. the control group; $^{*}p < 0.05$, $^{**}p < 0.01$, and $^{***}p < 0.001$ vs. TNF-α/IFN-γ-stimulated group.

2.7. AA involving in skin inflammation by alleviating the TWEAK/FN14 pathway in vivo and in vitro

The interplay between tumor necrosis factor-like weak inducer of apoptosis (TWEAK) and its receptor, fibroblast growth factor-inducible 14 (Fn14), plays an imperative role in assorted forms of skin inflammation, notably cutaneous autoimmune diseases, psoriasis, and AD [18]. We scrutinized alterations in TWEAK/FN14 levels through Western blotting and IHC analyses. In human keratinocytes, markedly elevated levels of TWEAK and FN14 induced by TNF-α/IFN-γ stimulation were significantly attenuated by both DEX and AA treatments (Fig. 7A). In murine models, TWEAK expression significantly escalated in the DNCB group, whereas AA-treated groups exhibited significant reductions surpassing those of the control group (Fig. 7B). Subsequent IHC experiments validated histological changes in TWEAK and FN14 expression (Fig. 7C). Notably, intense brown staining indicative of heightened expression appeared prominently in the epidermal and dermal layers of the DNCB-stimulated group, whereas expression notably decreased in both DEX- and AA-treated groups. These expression patterns align with previous studies [19,20].

3. Discussion

AD represents a chronic, recurring inflammatory skin condition characterized by complex interactions among the immune system, allergic responses, and skin barrier integrity [21]. This investigation delves into the effectiveness of AA therapy in managing AD symptoms by targeting STAT6 and subsequent TSLP expression in mouse skin tissues and keratinocytes, coupled with the modulation of the MAPK-related signaling cascade and Th2 cell differentiation.

IgE hyperactivity stands as an essential aspect in AD pathogenesis, correlating with acute skin manifestations, chronic excoriation, and exacerbation of pruritus [22]. Mast cell actuation triggered by IgE crosslinking prompts the emission of inflammatory mediators, fostering allergen hypersensitivity and abnormal immune reactions [23]. Notably, AA administration atopic dorsal skin mitigated mast cell infiltration and serum IgE levels (Figs. 2C, F, and 3A). Moreover, AA treatment alleviated AD severity, immune organ metrics, and dermatitis indices, including TEWL values and hyperkeratosis severity (Figs. 1 and 2).

Another significant facet contributing to AD pathogenesis is the dysregulated balance of Th1/Th2 cytokines, fostering TSLP, IL-4, IL-13, IL-5, and IL-10 secretion [24,25]. TNF-α, IL-6, and TARC, as typical pro-inflammatory cytokines and chemokines, stimulate monocyte recruitment and immune cell aggregation at inflammation sites, thereby fostering Th2 cell and group 2 innate lymphoid cell differentiation [26,27]. In particular, the release of IL-6 stimulates the secretion of IL-4 and IL-13 and the production of Th2-related cytokines, causing the occurrence of allergic inflammation in both human and murine models [28,29]. This study demonstrates AA

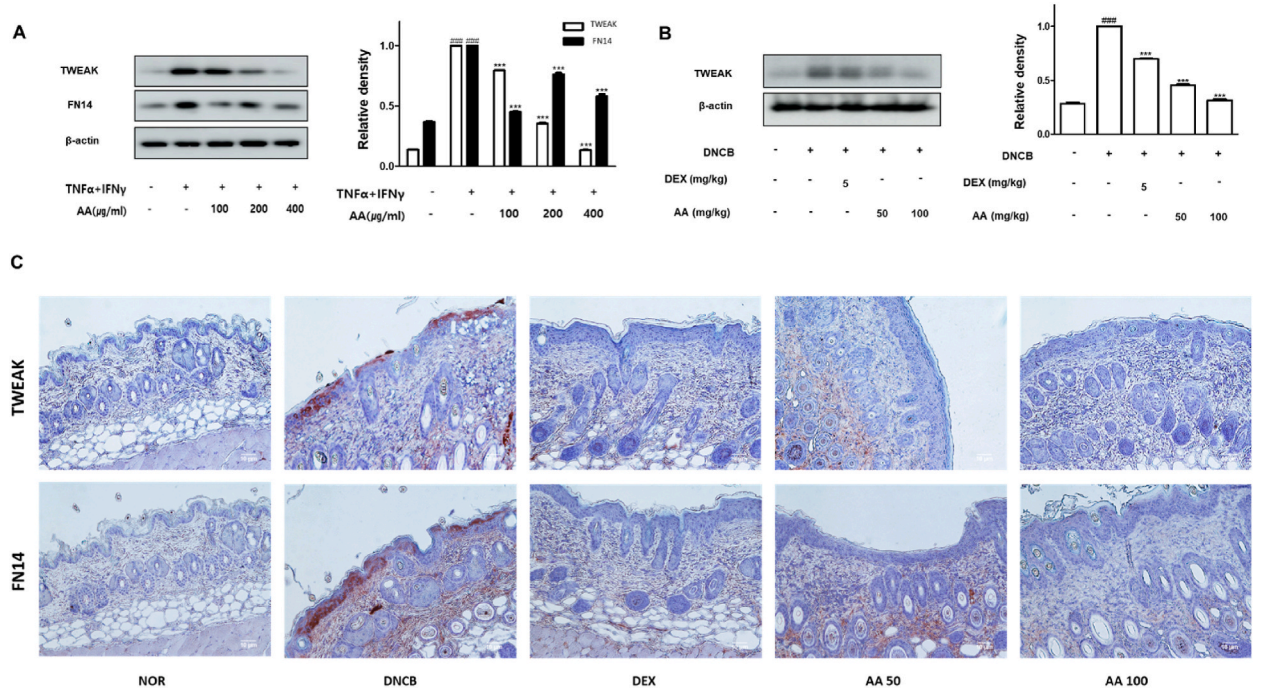

Fig. 7. Impact of AA on TWEAK/FN14 pathway *in vivo* and *in vitro* models.
The protein levels of (A) TWEAK/FN14 *in vitro* and (B) TWEAK *in vivo* were assessed via Western blot analysis using specific antibodies, with β-actin serving as the internal control. The quantification of protein expression was performed by measuring the band intensity relative to the corresponding β-actin form. (C) Histologic sections of skin dorsal tissue were immunohistochemically stained with TWEAK or FN14 antibody (scale bar = 10 μm). Data are presented as the mean ± standard deviation from three independent experiments. Statistical significance was determined as follows: $^{###}p < 0.001$ vs. the control group; $^{***}p < 0.001$ vs. TNF-α/IFN-γ-stimulated group or DNCB-treated group.

treatment's efficacy in reducing IL-6, IL-4, IL-13, and TARC expression *in vivo* and TNF-α levels *in vitro* (Figs. 3 and 5B). Upon binding of IL-4 or IL-13 to either type I or II IL-4 receptor complex, STAT6 undergoes phosphorylation and activation, culminating in increased periostin gene expression, a pro-inflammatory extracellular matrix protein with trophic roles in keratinocytes for TSLP production, as discussed elsewhere [17,30]. Here, we observed that AA treatment mitigated STAT6 protein expression by diminishing IL-6, IL-4, and IL-13 expression in both *in vivo* and *in vitro* models (Figs. 4D and 6D).

Following the reduction in STAT6 expression due to AA treatment, there was a significant inhibition of TSLP expression observed both *in vivo* and *in vitro* (Figs. 3C, 4D, 5C, and 6D). As a pivotal regulator of allergic inflammation, TSLP is primarily synthesized by keratinocytes, triggered by mechanical injury and protease-activated receptor 2 activation [5]. The TSLP receptor, a heterodimer of IL-7Rα and TSLPR, is manifested in miscellaneous immune cells such as Th2 cells, dendritic cells, mast cells, and type 2 innate lymphoid cells, playing a vital role in promoting Th2 cell differentiation in conjunction with TSLP [31]. Moreover, epithelial-derived TSLP modulates dendritic cell function, fostering Th2 responses through TARC production [32]. It also upregulates IgE expression levels and eosinophil counts by activating B cells through the excretion of IL-4, IL-5, and IL-13. Overexpression of TSLP in keratinocytes exacerbates pruritus-induced scratching, further promoting Th2 responses and contributing to skin barrier dysfunction through the itch-scratch cycle [33]. Consequently, AA treatment appears to restore filaggrin function *in vitro* (Fig. 6E) and sequentially influences Th2 responses by reducing TSLP expression, thereby impacting overall outcomes.

Additionally, MAPKs serve as pivotal regulators of inflammatory cytokines in keratinocytes, playing a crucial role in modulating inflammatory responses [34]. The mammalian MAPK family encompasses three subfamilies: ERK, JNK, and p38 MAPKs. This signaling cascade orchestrates essential cellular activities such as cell survival, proliferation, mobility, gene expression, and apoptosis. As linear kinase cascades, MAPK kinases (MAPKKs) activate MAPKs, such as SEK1/MKK4-JNK [26], as depicted in Fig. 6C. Our study elucidated that AA treatment elicits anti-inflammatory effects by suppressing ERK and JNK activity in both *in vivo* and *in vitro* models (Figs. 4C and 6C).

The TWEAK pathway and its receptor FN14 are emerging as promising targets for novel therapeutics in skin inflammation, including conditions like psoriasis and AD [35]. As noted earlier, AD is a representative chronic inflammatory skin disorder primarily driven by dysregulated Th2 immune responses. In AD, numerous pro-inflammatory cytokines and chemokines are released, accompanied by the assemblage of infiltrating immune cells [21,36]. These cytokines, such as TNF-α, IL-13, and CCL17 (TARC), interact with TWEAK, leading to the activation of keratinocytes and subsequent exhibition of pro-inflammatory mediators like TNF-α, IL-6, IL-13, interferon-γ, TARC, and TSLP [18,20], The impact of AA application on the expression of these mediators was observed in our study (Figs. 3 and 5). Recent research has shown the presence of TWEAK and FN14 in various experimental AD models, both *in vitro*, *in vivo*, and in patient skin lesions [19,20,37,38]. Consistent with previous findings, our study demonstrated an increase in TWEAK/FN14 expression in both the keratinocyte and AD mouse models, with a reduction effect evident upon AA treatment (Fig. 7). The TWEAK/FN14 pathway also facilitate swift phosphorylation of IκBα for NF-κB nuclear translocation in keratinocytes [39].Our experiment confirmed the result (Fig. 4B), suggesting that AA treatment alleviates skin inflammation via the TWEAK/FN14 pathway. Further correlation studies with TNF receptors are warranted to elucidate mechanistic insights.

In our investigation, AA exhibited notable efficacy in regulating TSLP, extending prior findings. The interplay between epithelial cells and innate immune cells via TSLP is implicated in driving AD and the "atopic march" phenomenon [40,41]. Additionally, timosaponin A-III, a major constituent of AA, has been shown to alleviate lung inflammation and autophagy in lung cancer cells [42,43], hinting at AA's potential to inhibit the atopic march. Furthermore, AA-derived components have shown significant effects on skin aging by improving skin thickness, reducing wrinkles, maintaining collagen fiber balance, and enhancing extracellular matrix dynamics [44,45]. Given the role of TSLP in collagen synthesis in keloid tissues [46], AA's ability to regulate TSLP expression and restore collagen synthesis suggests potential implications for improving skin elasticity and treating atopic conditions.

In this way, previous studies have established the safety and skin efficacy of AA and its active components. Building upon this foundation, the authors have explored the potential of AA in ameliorating AD through efficacy research. However, AD is an exceedingly intricate condition, and while the NC/Nga murine model utilized in this paper is tailored for a particular genetic mutant associated with AD, it may not fully mirror human AD. Moreover, the HaCaT keratinocyte model has restrictions in perfectly mimicking the complex composition of human skin. To address these constraints, employing diverse animal and cellular models in varied settings is imperative, complemented by clinical trials for human application. Furthermore, subsequent research is deemed necessary to investigate changes in gene expression and elucidate key biological signalling pathways through transcriptomic analysis following the application of AA, providing a detailed mechanism of action of AA.

4. Conclusions

This study demonstrates that AA treatment is a potential alternative for managing AD, representative skin inflammation, due to its anti-inflammatory effects and ability to improve the skin barrier function. *In vivo* and *in vitro*, AA treatment reduced the AD-like skin symptoms, such as skin barrier dysfunction and pruritus, by modulating the expression of pro-inflammatory mediators underlying the inhibition of STAT6/TSLP activation, NF-κB/MAPK-related pathways, and TWEAK/FN14 pathways.

5. Materials and methods

5.1. Preparation of AA extract

The dried roots of *Anemarrhena asphodeloides* were purchased from Nanum herb (Yeongchen, Gyeongbuk, Korea). The sample (200

g) was extracted by immersing it in 2 L of 70 % aqueous EtOH for 4 h. The extract was filtered and concentrated using a rotary vacuum evaporator (EYELA, Tokyo, Japan). Then, the sample was freeze-dried in vacuum using a freeze dryer (FDU-1200, EYELA, Tokyo, Japan) and stored in the freezer at −20 °C until analysis. Approximately 65.72 g of extract (at a concentration of 50 μg/mL) was obtained from 200 g of AA. The yield of the dried extract from the starting crude material was 32.86 %. For the *in vitro* experiment, the extract powder, which was the product of the drying process, was dissolved in distilled water.

5.2. Chemicals and reagents

The following materials were used in the study: Dimethyl sulfoxide (DMSO), DEX (lot #: BCCC1349), and 1-chloro-2,4-dinitrofluorobenzene (DNCB, lot #: MKBH8668V), all obtained from Sigma-Aldrich (St. Louis, MO, USA). Dulbecco's modified Eagle medium (DMEM), fetal bovine serum (FBS), penicillin, and streptomycin were sourced from Life Technologies Corporation (Grand Island, NY, USA). The MTT reagent, 3-(4,5-dimethylthiazol-2-yl)-2,5-diphenyl tetrazolium bromide, was acquired from Sigma Chemical Co. (St. Louis, MO, USA). Enzyme-linked immunosorbent assay (ELISA) kits used for determining levels of IgE, interleukin (IL)-6, thymic stromal lymphopoietin (TSLP), and TNF-α were sourced from R&D Systems, Inc. (Minneapolis, MN, USA). PowerUp™ SYBR® Green Master Mix was purchased from Applied Biosystems (Foster City, CA, USA). Oligonucleotide primers for IL-4, IL-13, thymus and activation-regulated chemokine (TARC), and GAPDH were provided by Bioneer Corporation (Daejeon, Chungbuk, Korea). PowerUp™ SYBR® Green Master Mix was procured from Applied Biosystems (Foster City, CA, USA). IL-4, IL-13, thymus and activation-regulated chemokine (TARC), and GAPDH oligonucleotide primers were sourced from Bioneer Corporation (Daejeon, Chungbuk, Korea). Primary antibodies for extracellular signal-regulated kinase (ERK; #9102), phosphorylated c-Jun N-terminal kinase (JNK) (#9251), JNK (# 9252), p-STAT6 (#56554), STAT6 (#9362), p-SAPK/Erk kinase (SEK1)/mitogen-activated protein kinase kinase 4 (MKK4) (#9156), SEK1/MKK4 (#9152), p-IκB (# 9246), IκB (#9242), and p-transforming growth factor beta-activated kinase 1 (TAK1) (#9339) were purchased from Cell Signaling Technology, Inc. (Danvers, MA, USA). Santa Cruz Biotechnology, Inc. (Santa Cruz, CA, USA) supplied the primary antibodies against p-ERK (sc-7383), TAK1 (sc-7967), filaggrin (sc-66192), β-actin (sc-81178), and peroxidase-conjugated secondary antibodies. Additionally, the primary antibodies against TSLP (cat. no. ab188766), TWEAK (ab37170), and FN14 (ab109365) were obtained from Abcam (Cambridge, UK).

5.3. Animal models

Male NC/Nga mice (weighing 24–26 g, aged 16–18 weeks) were sourced from Dae Han Bio Link Co. (Daejeon, Korea). The animals were housed under standard conditions with unrestricted access to food and water: 22–25 °C temperature, 40%–60 % humidity, and a 12/12 h light/dark cycle. After a one-week acclimatization period, the dorsal fur of the mice was shaved using an electric shaver. At random, the mice were divided into five groups, each consisting of 6–7 mice: (1) a baseline-applied normal group (normal control, NC), (2) a DNCB-sensitized group (DNCB), (3) a DNCB-sensitized and DEX-treated group (positive control), and (4–5) DNCB-sensitized groups topically treated with either 50 or 100 mg/kg of AA. To create AD-like skin lesions, 1 % DNCB dissolved in an acetone and corn oil mixture (3:1 v/v) was applied topically to the shaved dorsal skin (200 μL) and right ear (100 μL) twice during the first week. Subsequently, 0.4 % DNCB dissolved in the same acetone and corn oil mixture was applied to the same areas of the dorsal skin (150 μL) and right ear (50 μL) three times per week for 3 weeks. Four hours after each DNCB treatment, the mice were administered DEX (5 mg/kg mixed in Vaseline) or AA extract (50 or 100 mg/kg mixed in Vaseline) topically, once daily, during weekdays for 3 weeks. At the end of the experiment, the mice were sacrificed, blood samples were collected via the orbital sinus, and skin tissues were harvested for histological analysis. The experimental protocol is illustrated in Fig. 1A.

5.4. Evaluation of dermatitis severity

The dermatitis score was evaluated once a week through the Merkmal symptom scoring system, as outlined by Sone et al. [47]. The severity of symptoms, including edema, scarring/dryness, erythema/hemorrhage, and excoriation/erosion, was rated on a scale: 0 for none, 1 for mild (<20 %), 2 for moderate (20%–60 %), and 3 for severe (>60 %). The total dermatitis score was calculated by summing the individual scores.

5.5. Trans-epidermal water loss

Since a healthy skin barrier aids in retaining moisture and preventing water loss, epidermal water loss was assessed using the gpskin barrier light device (GPower, Seoul, Korea). On the final day of the experiment, TEWL was measured on the dorsal skin with the gpskin device immediately before euthanizing the mice.

5.6. Histological analysis

Following euthanasia, skin samples from the dorsal region were collected. These samples were fixed in 10 % buffered formalin and then embedded in paraffin. Sections of 8 μm thickness were prepared and stained with hematoxylin and eosin (H&E). Pathological features, including hyperkeratosis, dermal edema, epidermal and dermal hyperplasia, vesicular formation, parakeratosis, and inflammation, were examined. For evaluating mast cell infiltration, sections were stained with toluidine blue, and mast cell density per mm^2 was determined based on the average mast cell count in each specimen. Images were taken using an optical microscope (Leica,

Wetzlar, Germany) with Leica software. For IHC staining, the paraffin-embedded slides were first deparaffinized and then blocked with 0.6 % H_2O_2 in 50 % methanol to inhibit endogenous peroxidase activity. After treatment with 0.3 % Triton X-100 in phosphate-buffered saline, the slides were pre-blocked with 10 % normal goat serum for 1 h and subsequently incubated overnight at 4 °C with a specific antibody The following day, after washing, slides were incubated with horseradish peroxidase-conjugated secondary antibodies for 1 h. The slides were then treated with 3,3-diaminobenzidine chromogen and counterstained with H&E. Histological observations of the stained skin sections were made using a DM IL LED microscope (Leica Microsystems, Wetzlar, Germany), and images were captured with a DFC295 camera (Leica Microsystems). Digital images from each slide were analyzed using Leica Application Suite (Leica Microsystems).

5.7. Cytokine analysis

Serum from the collected blood was obtained by centrifugation at 1700×*g* for 30 min and then stored at −70 °C until further analysis. To measure serum levels of IgE and TSLP, mouse-specific ELISA kits (BD OptEIATM, BD Science, CA, USA) were utilized following the manufacturer's instructions. Protein extracts from the dorsal skin were prepared using PRO-PREP™ protein extraction solution (Intron Biotechnology Inc., Seoul, Korea) and incubated for 20 min at 4 °C. Afterward, the mixture was centrifuged at 11,000×*g* for 30 min at 4 °C to remove debris, and the supernatant was quickly frozen. Protein concentration was quantified using the Bio-Rad protein assay reagent (Bio-Rad Laboratories Inc., Hercules, CA, USA) in accordance with the manufacturer's guidelines. IL-6 levels were measured using an ELISA kit (BD OptEIATM, BD Science, CA, USA) as per the manufacturer's protocol. After Culture media, collected about 24 h post-AA treatment, were stored at −70 °C. TNF-α and TSLP expression levels were determined using human ELISA kits (BD OptEIATM, BD Science, CA, USA) according to the provided protocol.

5.8. Measurement of relative mRNA expression level using quantitative reverse transcription polymerase chain reaction

Using an RNeasy Fibrous Tissue Mini Kit (Qiagen, Valencia, CA), total RNA was isolated from the back skin tissue following the manufacturer's instructions. cDNA synthesis was performed with 2 μg of the extracted RNA, d(T)16 primer, and AMV reverse transcriptase. RT-PCR was carried out with SYBR Premix Ex Taq on a 7500 Real-Time PCR System (Applied Biosystems, Foster City, CA, USA). The cDNA generated was approximately 200 bp in length. Gene expression levels were determined using the ΔΔCt method, with data normalized to GAPDH levels. Results were presented as the optical density ratio relative to GAPDH. The sequences of the primers used for real-time RT-PCR were as follows: mouse IL-4, forward 5′-ATCATCGGCATTTTGAACGAGGTC-3′ and reverse 5′-ACCTTGGAAGCCCTACAGACGA-3'; mouse IL-13, forward 5′-AACGGCAGCATGGTATGGAGTG-3′, and reverse 5′-TGGGTCCTGTAGATGGCATTGC-3'; mouse TARC, forward 5′-CGAGAGTGCTGCCTGGATTACT-3′, and reverse 5′-GGTCTGCACAGATGAGCTTGCC-3'; and mouse GAPDH, forward 5′-GACGGCCGCATCTTCTTGT-3′, and reverse 5′-CACACCGACCTTCACCATTTT-3'.

5.9. Western blot analysis

Protein extracts from both dorsal skin tissue and HaCaT cells were obtained using PRO-PREP™ protein extraction solution (Intron Biotechnology, Seoul, Korea), followed by homogenization at 4 °C. Afterward, the samples were then centrifuged at 11,000×*g* for 30 min at 4 °C to remove cellular debris, and the supernatant was quickly frozen. As per the manufacturer's protocol, Bio-Rad protein assay reagent was utilized to measure the protein concentrations. Proteins from each sample were separated by electrophoresis on an 8%–12 % SDS-polyacrylamide gel and then transferred onto a polyvinylidene difluoride (PVDF) membrane via electroblotting. For 30 min, the membranes were blocked with 2.5 % skim milk solution at room temperature, followed by overnight incubation with a primary antibody (1:1000 dilution in Tween 20/Tris-buffered saline (T/TBS)) at 4 °C. Following three washes with T/TBS, the blots were treated with a horseradish peroxidase-conjugated secondary antibody (1:2000 dilution) for 2 h at room temperature. The blots were washed again three times with T/TBS and visualized using an enhanced chemiluminescence system (GE Healthcare, WI, USA). Densitometric analysis was performed using Bio-Rad Quantity One software (version 4.3.0; Bio-Rad Laboratories, Inc.).

5.10. Cell culture and sample treatment

HaCaT keratinocytes were generously provided by Prof. Kyung-Tae Lee (Kyung Hee University, Seoul, Korea). These cells were maintained at 37 °C in DMEM containing 10 % FBS, 100 U/mL penicillin, and 100 μg/mL streptomycin in a humidified environment with 5 % CO2. HaCaT keratinocytes were plated at a density of 1×10^5 cells/mL per well. After seeding, the cells were treated with AA at concentrations of 100, 200, or 400 μg/mL for 1 h, followed by stimulation with a mixture of TNF-α and IFN-γ (10 ng/mL each) for the designated duration.

5.11. Cell viability assay

Cell viability was estimated using the MTT colorimetric assay. HaCaT cells were plated at a density of 5×10^4 cells per well in a 96-well plate and allowed to incubate for 24 h. Afterward, the cells were exposed to various concentrations of AA in the culture medium and incubated for an additional 24 h. On the following day, 50 μL of MTT solution (5 mg/mL) was added to each well and incubated for 4 h. The resulting formazan crystals were dissolved in DMSO, and the absorbance was read at 540 nm with an Epoch microplate spectrometer (BioTek, Winooski, VT, USA).

5.12. Statistical analysis

Data are presented as the mean ± standard deviation from three independent experiments. Group comparisons were performed using a one-way analysis of variance (ANOVA), followed by Dunnett's post-hoc test, with the aid of GraphPad Prism 5 software (GraphPad Software, San Diego, CA, USA). Statistical significance was defined as a p-value of less than 0.05.

Ethical approval

This study involving animal subjects was reviewed and approved by the Institutional Animal Care and Use Committee (IACUC) of Sangji University, approval number: IACUC no. 2020-2, dated April.2020. The study was conducted following the Guidelines for the Care and Use of Laboratory Animals, 8th edition in 2011.

Funding Statement

This research was funded by the National Research Foundation of Korea (NRF) grant funded by the Korea government (No. NRF-2022R1A2C2093050) and Institute of Information & communications Technology Planning & Evaluation (IITP) under the Artificial Intelligence Convergence Innovation Human Resources Development (IITP-2024-RS-2023-00254592) grant funded by the Korea government (MSIT).

Data availability statement

Data has not been deposited into a publicly available repository. However, data will be made available upon request. Please contact corresponding author for access.

CRediT authorship contribution statement

Hye-Min Kim: Writing – review & editing, Writing – original draft, Visualization, Investigation, Formal analysis, Data curation, Conceptualization. **Yun-Mi Kang:** Writing – review & editing, Validation, Methodology, Conceptualization. **Bo-Ram Jin:** Writing – review & editing, Validation. **Minho Lee:** Validation, Supervision, Funding acquisition. **Hyo-Jin An:** Writing – review & editing, Validation, Supervision.

Declaration of competing interest

The authors declare that they have no known competing financial interests or personal relationships that could have appeared to influence the work reported in this paper.

Acknowledgement

This work was supported by Sangji University Graduate School and also supported by KREONET (Korea Research Environment Open NETwork) which is managed and operated by KISTI (Korea Institute of Science and Technology Information).

References

[1] D.Y. Jeong, M.S. Ryu, H.J. Yang, S.Y. Jeong, T. Zhang, H.J. Yang, M.J. Kim, S. Park, Pediococcus acidilactici intake decreases the clinical severity of atopic dermatitis along with increasing mucin production and improving the gut microbiome in Nc/Nga mice, Biomedicine & pharmacotherapy = Biomedecine & pharmacotherapie 129 (2020) 110488.
[2] W. Frazier, N. Bhardwaj, Atopic dermatitis: diagnosis and treatment, Am. Fam. Physician 101 (10) (2020) 590–598.
[3] E. Nettis, M. Ortoncelli, G. Pellacani, C. Foti, E. Di Leo, C. Patruno, F. Rongioletti, G. Argenziano, S.M. Ferrucci, L. Macchia, et al., A multicenter study on the prevalence of clinical patterns and clinical phenotypes in adult atopic dermatitis, Journal of investigational allergology & clinical immunology 30 (6) (2020) 448–450.
[4] Y. Kohara, K. Tanabe, K. Matsuoka, N. Kanda, H. Matsuda, H. Karasuyama, H. Yonekawa, A major determinant quantitative-trait locus responsible for atopic dermatitis-like skin lesions in NC/Nga mice is located on Chromosome 9, Immunogenetics 53 (1) (2001) 15–21.
[5] K. Kabashima, New concept of the pathogenesis of atopic dermatitis: interplay among the barrier, allergy, and pruritus as a trinity, J. Dermatol. Sci. 70 (1) (2013) 3–11.
[6] E.Y. Zhang, A.Y. Chen, B.T. Zhu, Mechanism of dinitrochlorobenzene-induced dermatitis in mice: role of specific antibodies in pathogenesis, PLoS One 4 (11) (2009) e7703.
[7] M. Boguniewicz, D.Y. Leung, Atopic dermatitis: a disease of altered skin barrier and immune dysregulation, Immunol. Rev. 242 (1) (2011) 233–246.
[8] D.J. Kwon, Y.S. Bae, S.M. Ju, A.R. Goh, G.S. Youn, S.Y. Choi, J. Park, Casuarinin suppresses TARC/CCL17 and MDC/CCL22 production via blockade of NF-kappaB and STAT1 activation in HaCaT cells, Biochemical and biophysical research communications 417 (4) (2012) 1254–1259.
[9] T.Y. Gil, C.H. Hong, H.J. An, Anti-inflammatory effects of ellagic acid on keratinocytes via MAPK and STAT pathways, Int. J. Mol. Sci. 22 (3) (2021).
[10] E. Guttman-Yassky, J.M. Hanifin, M. Boguniewicz, A. Wollenberg, R. Bissonnette, V. Purohit, I. Kilty, A.M. Tallman, M.A. Zielinski, The role of phosphodiesterase 4 in the pathophysiology of atopic dermatitis and the perspective for its inhibition, Experimental dermatology 28 (1) (2019) 3–10.
[11] T. Torres, E.O. Ferreira, M. Goncalo, P. Mendes-Bastos, M. Selores, P. Filipe, Update on atopic dermatitis, Acta medica portuguesa 32 (9) (2019) 606–613.
[12] Y. Lin, W.R. Zhao, W.T. Shi, J. Zhang, K.Y. Zhang, Q. Ding, X.L. Chen, J.Y. Tang, Z.Y. Zhou, Pharmacological activity, pharmacokinetics, and toxicity of timosaponin aiii, a natural product isolated from Anemarrhena asphodeloides Bunge: a review, Front. Pharmacol. 11 (2020) 764.

[13] S. Zhang, Q. Zhang, L. An, J. Zhang, Z. Li, J. Zhang, Y. Li, M. Tuerhong, Y. Ohizumi, J. Jin, et al., A fructan from Anemarrhena asphodeloides Bunge showing neuroprotective and immunoregulatory effects, Carbohydrate polymers 229 (2020) 115477.
[14] H.S. Kim, J.H. Song, U.J. Youn, J.W. Hyun, W.S. Jeong, M.Y. Lee, H.J. Choi, H.K. Lee, S. Chae, Inhibition of UVB-induced wrinkle formation and MMP-9 expression by mangiferin isolated from Anemarrhena asphodeloides, Eur. J. Pharmacol. 689 (1–3) (2012) 38–44.
[15] A.R. Im, Y.K. Seo, S.H. Cho, K.H. O, K.M. Kim, S. Chae, Clinical evaluation of the safety and efficacy of a timosaponin A-III-based antiwrinkle agent against skin aging, J. Cosmet. Dermatol. 19 (2) (2020) 423–436.
[16] Y.M. Kang, K.Y. Lee, H.J. An, Inhibitory effects of helianthus tuberosus ethanol extract on dermatophagoides farina body-induced atopic dermatitis mouse model and human keratinocytes, Nutrients 10 (11) (2018).
[17] M. Newsom, A.M. Bashyam, E.A. Balogh, S.R. Feldman, L.C. Strowd, New and emerging systemic treatments for atopic dermatitis, Drugs 80 (11) (2020) 1041–1052.
[18] Q. Liu, S. Xiao, Y. Xia, TWEAK/Fn14 activation participates in skin inflammation, Mediat. Inflamm. (2017) 6746870.
[19] Q. Liu, H. Wang, X. Wang, M. Lu, X. Tan, L. Peng, F. Tan, T. Xiao, S. Xiao, Y. Xia, Experimental atopic dermatitis is dependent on the TWEAK/Fn14 signaling pathway, Clin. Exp. Immunol. 199 (1) (2020) 56–67.
[20] M. Zimmermann, A. Koreck, N. Meyer, T. Basinski, F. Meiler, B. Simone, S. Woehrl, K. Moritz, T. Eiwegger, P. Schmid-Grendelmeier, et al., TNF-like weak inducer of apoptosis (TWEAK) and TNF-alpha cooperate in the induction of keratinocyte apoptosis, The Journal of allergy and clinical immunology 127 (1) (2011) 200–207, 207 e201-210.
[21] H. Li, Z. Zhang, H. Zhang, Y. Guo, Z. Yao, Update on the pathogenesis and therapy of atopic dermatitis, Clin. Rev. Allergy Immunol. 61 (3) (2021) 324–338.
[22] M.J. Lavery, M.O. Kinney, H. Mochizuki, J. Craig, G. Yosipovitch, Pruritus: an overview. What drives people to scratch an itch? Ulster Med. J. 85 (3) (2016) 164–173.
[23] J. Ye, H. Piao, J. Jiang, G. Jin, M. Zheng, J. Yang, X. Jin, T. Sun, Y.H. Choi, L. Li, et al., Polydatin inhibits mast cell-mediated allergic inflammation by targeting PI3K/Akt, MAPK, NF-kappaB and Nrf2/HO-1 pathways, Sci. Rep. 7 (1) (2017) 11895.
[24] J.M. Spergel, E. Mizoguchi, H. Oettgen, A.K. Bhan, R.S. Geha, Roles of TH1 and TH2 cytokines in a murine model of allergic dermatitis, The Journal of clinical investigation 103 (8) (1999) 1103–1111.
[25] S.H. Kim, G.S. Seong, S.Y. Choung, Fermented Morinda citrifolia (noni) alleviates DNCB-induced atopic dermatitis in NC/nga mice through modulating immune balance and skin barrier function, Nutrients 12 (1) (2020).
[26] H. Ichijo, From receptors to stress-activated MAP kinases, Oncogene 18 (45) (1999) 6087–6093.
[27] J.H. Yang, Y.H. Hwang, M.J. Gu, W.K. Cho, J.Y. Ma, Ethanol extracts of Sanguisorba officinalis L. suppress TNF-alpha/IFN-gamma-induced pro-inflammatory chemokine production in HaCaT cells, Phytomedicine : international journal of phytotherapy and phytopharmacology 22 (14) (2015) 1262–1268.
[28] M.H. Kaplan, U. Schindler, S.T. Smiley, M.J. Grusby, Stat6 is required for mediating responses to IL-4 and for development of Th2 cells, Immunity 4 (3) (1996) 313–319.
[29] S. Goenka, M.H. Kaplan, Transcriptional regulation by STAT6, Immunol. Res. 50 (1) (2011) 87–96.
[30] H. Harb, T.A. Chatila, Mechanisms of dupilumab, Clin. Exp. Allergy : journal of the British Society for Allergy and Clinical Immunology 50 (1) (2020) 5–14.
[31] Y. Zhang, B. Zhou, Functions of thymic stromal lymphopoietin in immunity and disease, Immunol. Res. 52 (3) (2012) 211–223.
[32] C.C. Hui, D.M. Murphy, H. Neighbour, M. Al-Sayegh, S. O'Byrne, B. Thong, J.A. Denburg, M. Larche, T cell-mediated induction of thymic stromal lymphopoietin in differentiated human primary bronchial epithelial cells, Clin. Exp. Allergy : journal of the British Society for Allergy and Clinical Immunology 44 (7) (2014) 953–964.
[33] Y. Li, W. Wang, Z. Lv, Y. Li, Y. Chen, K. Huang, C.J. Corrigan, S. Ying, Elevated expression of IL-33 and TSLP in the airways of human asthmatics in vivo: a potential biomarker of severe refractory disease, Journal of immunology 200 (7) (2018) 2253–2262.
[34] R.B. Kjellerup, K. Kragballe, L. Iversen, C. Johansen, Pro-inflammatory cytokine release in keratinocytes is mediated through the MAPK signal-integrating kinases, Experimental dermatology 17 (6) (2008) 498–504.
[35] X. Wang, S. Xiao, Y. Xia, Tumor necrosis factor receptor mediates fibroblast growth factor-inducible 14 signaling, Cell. Physiol. Biochem. : international journal of experimental cellular physiology, biochemistry, and pharmacology 43 (2) (2017) 579–588.
[36] A. Schabitz, K. Eyerich, N. Garzorz-Stark, So close, and yet so far away: the dichotomy of the specific immune response and inflammation in psoriasis and atopic dermatitis, Journal of internal medicine 290 (1) (2021) 27–39.
[37] H.R. Nada, L.A. Rashed, A.M. Mohamed, H.A. Abdelkader, Tumor necrosis factor-like weak inducer of apoptosis (TWEAK) in psoriasis and atopic dermatitis: a case-control study, J. Am. Acad. Dermatol. 84 (6) (2021) 1707–1708.
[38] D. Sidler, P. Wu, R. Herro, M. Claus, D. Wolf, Y. Kawakami, T. Kawakami, L. Burkly, M. Croft, TWEAK mediates inflammation in experimental atopic dermatitis and psoriasis, Nat. Commun. 8 (2017) 15395.
[39] L. Jin, A. Nakao, M. Nakayama, N. Yamaguchi, Y. Kojima, N. Nakano, R. Tsuboi, K. Okumura, H. Yagita, H. Ogawa, Induction of RANTES by TWEAK/Fn14 interaction in human keratinocytes, J. Invest. Dermatol. 122 (5) (2004) 1175–1179.
[40] S.F. Ziegler, F. Roan, B.D. Bell, T.A. Stoklasek, M. Kitajima, H. Han, The biology of thymic stromal lymphopoietin (TSLP), Advances in pharmacology 66 (2013) 129–155.
[41] T.P. Moran, B.P. Vickery, The epithelial cell-derived atopic dermatitis cytokine TSLP activates neurons to induce itch, Pediatrics 134 (Suppl 3) (2014) S160–S161.
[42] B.K. Park, K.S. So, H.J. Ko, H.J. Kim, K.S. Kwon, Y.S. Kwon, K.H. Son, S.Y. Kwon, H.P. Kim, Therapeutic potential of the rhizomes of Anemarrhena asphodeloides and timosaponin A-III in an animal model of lipopolysaccharide-induced lung inflammation, Biomolecules & therapeutics 26 (6) (2018) 553–559.
[43] J. Liu, X. Deng, X. Sun, J. Dong, J. Huang, Inhibition of autophagy enhances timosaponin AIII-induced lung cancer cell apoptosis and anti-tumor effect in vitro and in vivo, Life Sci. 257 (2020) 118040.
[44] Y. Wang, Y. Dan, D. Yang, Y. Hu, L. Zhang, C. Zhang, H. Zhu, Z. Cui, M. Li, Y. Liu, The genus Anemarrhena Bunge: a review on ethnopharmacology, phytochemistry and pharmacology, J. Ethnopharmacol. 153 (1) (2014) 42–60.
[45] J. Zhu, Z. Wang, F. Chen, Association of key genes and pathways with atopic dermatitis by bioinformatics analysis, Med. Sci. Mon. Int. Med. J. Exp. Clin. Res. : international medical journal of experimental and clinical research 25 (2019) 4353–4361.
[46] J.U. Shin, S.H. Kim, H. Kim, J.Y. Noh, S. Jin, C.O. Park, W.J. Lee, D.W. Lee, J.H. Lee, K.H. Lee, TSLP is a potential initiator of collagen synthesis and an activator of CXCR4/SDF-1 Axis in keloid pathogenesis, J. Invest. Dermatol. 136 (2) (2016) 507–515.
[47] K. Sone, T. Yamamoto-Sawamura, S. Kuwahara, K. Nishijima, T. Ohno, H. Aoyama, S. Tanaka, Changes of estrous cycles with aging in female F344/n rats, Experimental animals 56 (2) (2007) 139–148.